High-resolution laser photoionization spectroscopy of radioactive europium isotopes[1)]

A. N. Zherikhin, O. N. Kompanets, V. S. Letokhov, V. I. Mishin, and V. N. Fedoseev

Institute of Spectroscopy, Academy of Sciences of the USSR

G. D. Alkhazov, A. E. Barzakh, E. E. Berlovich, V. P. Denisov, A. G. Dernyatin,
and V. S. Ivanov

B. P. Konstantinov Institute of Nuclear Physics, Academy of Sciences of the USSR, Leningrad

A study is made of the autoionization spectrum for transitions of the Eu atom from excited states. The most efficient schemes are found for the three-step laser photoionization of Eu atoms. The data are used for measurement of the isotope shifts in the optical spectrum of the radioactive isotopes of Eu at the laser-nuclear complex at the Leningrad Institute of Nuclear Physics and the Institute of Spectroscopy. On the basis of the measured isotope shifts we have determined for the first time the changes in the mean-square distribution of nuclear charge for the radioactive isotopes $^{150\text{-}145}$Eu. The prospects for improving the sensitivity of the method are discussed.

1. INTRODUCTION

Measurements of the isotope shifts and the hyperfine structure of atomic spectral lines permit one to determine such parameters of importance in nuclear physics as the change in the mean-square radius $\delta \langle r^2 \rangle$ of the charge distribution, the nuclear spin I, the magnetic dipole moment μ, and the electric quadrupole moment Q.

The methods of classical high-resolution atomic spectroscopy have been used to measure the isotope shifts and the hyperfine structure of the atomic lines of stable and certain long-lived radioactive nuclides. Recent technical progress in the production and mass-separation of radioactive nuclides and the use of high-resolution and high-sensitivity laser optical methods have now made it possible to make such measurements for long chains of radioactive isotopes, extending far beyond the beta-stability band of the nuclei and right up to the limits of nuclear stability.

The hyperfine structure and isotope shift are small effects is atomic spectra and are usually masked by the Doppler broadening of the spectral line. For studying these effects it is therefore necessary to use the methods of sub-Doppler spectroscopy, with a resolution $\lesssim 100$ MHz. In the case of radioactive nuclides the problem is complicated by the weakness of the flux of mass-separated isotopes produced in proton and ion accelerators and nuclear reactors. For example, at the ISOLDE complex at CERN, the flux of rare earth isotopes is at maximum 10^8–10^{11} atoms/sec and falls to 10^3–10^6 atoms/sec for isotopes with decay half-lives of the order of minutes.[2] In addition, in studying nuclides with short lifetimes one can use only highly sensitive methods capable of "on-line" operation with the source of the radioactive nuclides.

Long isotopic chains of the alkali elements from Na to Fr have been studied[3,4] by laser optical pumping of atoms in an atomic beam. The method of laser excitation of the fluorescence of atomic vapors in a cell has been used to study isotopes of mercury[5] and cadmium.[6] The hyperfine struc-

ture and isotope shifts of radioactive isotopes of Au have been investigated by measuring the refractive index of the vapor while scanning the laser frequency in the region of an atomic absorption line. Unstable isotopes of Ba and Pb have been studied by laser excitation of the fluorescence of atoms in an atomic beam.[8,9] Isotopes of Ba, Yb, Er, and Dy have been studied by excitation of the fluorescence of atoms in a fast beam by collinear laser radiation.[5,10] Detailed information on the study of nuclei by means of the hyperfine structure and isotope shifts and on newly developed methods can be found in the review by Otten[11] and in the Conference Proceedings.[12]

In the present paper we report the first study of the hyperfine structure and isotope shift of radioactive nuclides by multistep laser photoionization of atoms in an atomic beam, a method proposed and developed at the Institute of Spectroscopy (see reviews[13-16]). This method basically consists of the following. Laser radiation at several frequencies excites an atom sequentially from level to level. From the excited state the atom is also photoionized by the laser radiation. Because the intermediate transitions are resonance transitions, they are readily saturated. Here a large fraction, close to 100%, of the atoms turn out to be excited. An atom from the excited state can be efficiently ionized through either autoionization states[17] or Rydberg states.[18] The charged paticles—electrons and ions—which arise are easily detected at close to unit efficiency. The hyperfine structure and isotope shifts of the absorption lines of one of the transitions are studied by tuning the laser frequency of the corresponding excitation step. The spectral width of the laser here should be smaller than the distance between the components of the hyperfine structure of the atomic line. It is convenient to choose the laser linewidths for the other excitation steps larger than the hyperfine structure of the remaining lines corresponding to these transitions.

The photoionization method of studying radioactive nuclei is the underlying principle of the IRIS system,[19-20] a laser-nuclear complex based on the proton accelerator and

0038-5646/84/040729-08$04.00   © 1985 American Institute of Physics   729

mass separator of the Leningrad Institute of Nuclear Physics and operated in cooperation with the Institute of Spectroscopy. It should be noted that the method which we have used is fundamentally different from other optical methods in that it not only enables one to study the hyperfine structure and isotope shifts but also to separate isotopes, isomers, and isobars by selectively ionizing them from the neutral state.

As the first objects of study we chose rare earth elements with nuclei close to the filled neutron shell with $N = 82$. Nuclei in this region are interesting objects of study for the following reasons: First, a systematic measurement of the charge radii of isotopic chains including magic nuclei (with $N = 82$) will elucidate the role of shell effects for neutron-deficient nuclei far from the β-stability band. Second, as the neutron number is increased from 82 to 90 the shape of the nucleus should change from spherical to highly deformed. The character of this change is of particular interest.[21,22] Finally, for $N < 82$ a new deformation region can exist.[23]

In Refs. 1 we report some preliminary data on the changes in the charge radii of certain neutron-deficient isotopes of europium; these radii were measured by the authors for the first time by the method of multistep laser photoionization of atoms. In the present paper we justify our choice for the optimum photoionization scheme for atoms of europium, describe the experimental techniques, give refined results for the measured isotope shifts for europium isotopes with mass numbers $A = 145$–149, and newly report the value of isotope shift for Eu with $A = 150$ and 151.

2. MULTISTEP LASER PHOTOIONIZATION SCHEME FOR EUROPIUM ATOMS

A high efficiency can be achieved in pulsed multistep laser photoionization in the most general case when the laser pulses of all the excitation steps act on an atom either simultaneously or with a delay shorter than the lifetime of the intermediate states.[24] The reason for this is that the intermediate levels of the atoms can have short lifetimes τ_k. The atoms excited to these levels will not be lost as a result of spontaneous transitions to other levels not belonging to the chosen excitation scheme if the duration τ_L of the laser pulses satisfy the condition $\tau_L \lesssim \tau_k$. Furthermore, pulsed lasers, owing to their high power, can saturate the atomic resonance transitions much more easily than can cw lasers. In order to intercept all the atoms in the beam as it crosses the region of interaction with the laser field, the laser pulse repetition frequency should be rather high (100 kHz).

Frequency-tunable dye lasers have been developed at the Institute of Spectroscopy[25,26] on the basis of pulsed copper-vapor lasers of Soviet manufacture (model ILGI-101), with a pulse repetition frequency of 10 kHz. These dye lasers, which form the heart of the laser-nuclear complex, are used for multistep photoionization of atoms. This complex is described later on. Here we shall give only the basic parameters needed in choosing the optimum photoionization scheme. The duration of the light pulses is $\tau_L = 18$ nsec, the lasing wavelength is tunable over the range from 540 to 700 nm, and the average radiation power is 300 mW.
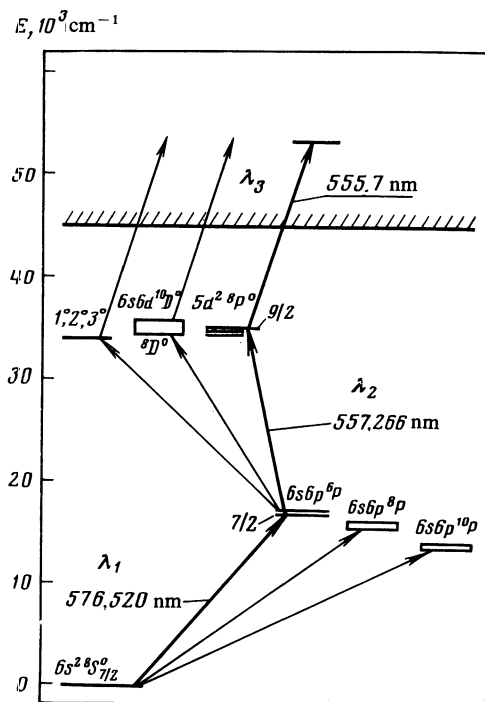

FIG. 1. Scheme of several atomic transitions in Eu I; the transitions used for the laser resonance photoionization of the radioactive isotopes are indicated by heavy arrows.

For europium and other lanthanides the best scheme is three-step ionization (for europium $E_i = 45734.9$ cm^{-1})[27] with radiation at the fundamental frequency of the lasers. Figure 1 shows a partial level scheme for Eu I. As the transition for the first excitation step one can choose the transitions from the ground state $6s^2\ {}^8S^0_{7/2}$ to the $6s6p\ {}^6P$, $6s6p\ {}^8P$, and $6s6p\ {}^{10}P$ states; these transitions have been studied for stable isotopes from the standpoint of hyperfine structure and isotope shifts. The wavelengths of the transitions to the levels of the ${}^8P$ and ${}^{10}P$ terms lie in the region 600–710 nm. If these transitions are used as the first excitation step, then one can implement a three-step excitation and ionization of europium atoms through Rydberg states by a method analogous to that which was used by the authors for photoionization of ytterbium atoms.[28] If, on the other hand, one uses for the first step the transition ${}^8S^0_{7/2}$–${}^6P_{7/2}$ ($\lambda_1 = 576.520$ nm) or ${}^8S^0_{7/2}$–${}^6P_{5/2}$ ($\lambda_1 = 564.580$ nm), then excitation of the atom to a Rydberg state would require radiation at a wavelength $\lambda_3 > 700$ nm. Efficient dyes lasing in this region under copper-laser pumping have yet to be found. Therefore, in this case the only applicable method of ionization is excitation of the atom to an autoionization state.

In choosing the first transition, at which the hyperfine structure and isotope are studied, it is necessary to consider the width of the hyperfine structure and the size of the isotope shift. For some of the above transitions this information is known.[29] The hyperfine structure of these transitions is governed mainly by the splitting of the upper level. For the $6s6p\ {}^6P_{5/2,7/2}$ states the width of the hyperfine structure is anomalously small (about 300 MHz) compared to the isotope shift between the stable isotopes ^{151}Eu and ^{153}Eu, which
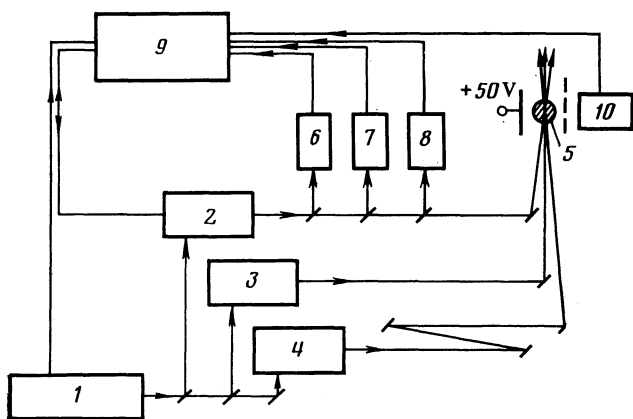
FIG. 2. Schematic of laser photoionization spectrometer used for measuring the saturation energy densities of the atomic transitions, the lifetimes of the states, and the energies of the Rydberg and autoionizing states: 1) pulsed nitrogen laser, 2, 3, 4) tunable dye lasers, 5) atomic beam, 6) Fabry-Perot interferometer, 7) neon hollow-cathode lamp, 8) monochromator, 9) computerized electronics complex, 10) secondary electron multiplier.

to some intermediate state by the radiation of two dye lasers tuned to resonance with the intermediate transitions. As the frequency of the third laser is scanned, the spectrum of the autoionization states is observed by detecting the photoions. The excitation and ionization of the atoms takes place in a collimated atomic beam which intersects the laser beams at right angles. The photoions are detected by a secondary electron multiplier.

The absolute values of the wavelengths of the transitions were measured by the following method. Part of the radiation of the continuously tunable laser is coupled out to a Fabry-Perot interferometer with a free-dispersion region of 1 cm^{-1} and to a neon hollow-cathode lamp. The electrode signals from the hollow-cathode lamp, the secondary electron multiplier, and a photodiode placed at the output of the interferometer were sent to a computerized measuring and calculating complex. The laser frequency v_x at which the photocurrent line due to excitation of an autoionization state appeared was determined by the formula

$$v_x = v_1 + \frac{v_2 - v_1}{n_{1-2}} n_{1x}, \qquad (1)$$

where v_1 and v_2 are the tabulated atomic transition frequencies for neon, n_{1-2} is the number of whole and fractional interference fringes which fit between the centers of the lines v_1 and v_2, and n_{1x} is the same, but for the lines v_1 and v_x. The accuracy with which the transition frequencies can be measured by this method is governed by the laser linewidth ($\Delta v_L = 0.3 \text{ cm}^{-1}$) or the atomic linewidth and by the nonuniformity of the frequency scanning of the laser. In our experiments the uncertainty was $\pm 0.1 \text{ cm}^{-1}$. Table I gives some of the strongest autoionization transitions observed in europium; these transitions were then used in experiments with radioactive Eu atoms.

The maximum ion yield during three-step laser photoionization of atoms is reached in the case in which all three transitions are saturated.[13] If, however, the energy parameters of the lasers do not permit saturation of all three transitions, one must find a sequence of transitions for which two of the transitions can be saturated and the third transition has a maximum excitation cross section. The oscillator

is $\Delta v(151-153) = 3619$ MHz (Ref. 29) for the line $\lambda_1 = 576.520$ nm. For this reason the excitation lines $\lambda_1 = 564.580$ nm and $\lambda_1 = 576.520$ nm are extemely convenient for measuring the isotope shifts, since it is not necessary to identify the components of the hyperfine structure and determine the centroid of the line. On the basis of these considerations we chose for the first excitation step one of the transitions with an anomalously small hyperfine structure. In this case the ionization of the atom can be effectively arranged only through the autoionization states.

The optimum photoionization scheme was chosen by the following program: 1) study the spectra for excitation to the autoionization states and choose the transitions with the largest cross section; 2) measure the saturation energies and lifetimes of the intermediate states from which the strongest autoionization resonances are reached; 3) measure the transition frequencies. For studying the high-lying and autoionization states of atoms a laser photoionization spectrometer consisting of three nitrogen-laser-pumped dye lasers was built at the Institute of Spectroscopy. The working principle of the spectrometer is as follows (Fig. 2). Atoms are excited

TABLE I. Strongest autoionization transitions observed in a three-step scheme for laser photoionization of Eu I. The first excitation step used the transition $4f^7 6s^2 \, ^8S^0_{7/2} \rightarrow 4f^7 6s6p \, ^6P_{7/2}$, $\lambda_1 = 576.520$ nm; λ_2 is the transition wavelength of the second excitation step; E_2 is the energy of the level from which the transition is observed to the autoionization state with energy E_a; and λ_a and v_a are the wavelength and frequency of the autoionization transitions.

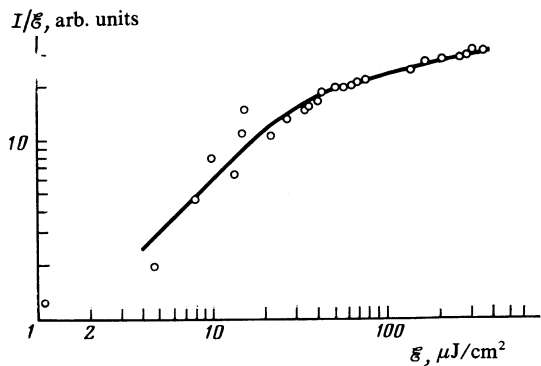| λ_2, nm	Excited state		v_a, cm^{-1}	λ_a, nm	E_a, cm^{-1}
	term	E_2, cm^{-1}			
595.578	$3^0_{7/2, \, 9/2}$	34126.42	14631	683.3	48757
597.739	$1^0_{5/2}$	34065.73	17067	585.8	51132
595.578	$3^0_{7/2, \, 9/2}$	34126.42	17153	582.8	51279
565.028	$^8D^0_{7/2}$	35033.98	16703	598.5	51737
557.266	$^8P^0_{9/2}$	35280.43	17990	555.7	53271
554.253	$^8D^0_{7/2}$	35377.94	17894	558.7	53272

I/ℰ, arb. units

FIG. 3. Ratio of photoion current to the energy density $\mathscr{E}$ of the laser radiation *versus* the energy density of the laser pulse at the transition between the excited states.

FIG. 4. Photoion current *versus* the optical delay time of the laser pulse of the third excitation step with respect to the second-step pulse.

strengths for the transtitions of the first excitation step are known,[30] and they are such that the transitions are easily saturated by the narrow-band emission of dye lasers pumped by a copper-vapor laser. The average saturation power density of these transitions is around 30 mW/cm².

There is a lack of data on the cross sections for transitions between excited states of europium. Therefore, for the series of intermediate transitions to states in which the strongest autoionization resonances were observed, the excitation cross sections were measured by the saturation method.[31] The saturation energy $\mathscr{E}_{sat}$ was determined by illuminating a beam of Eu atoms with two lasers. The frequency of the first laser was tuned to one of the first transitions of the excitation step, e.g., $^8S^0_{7/2}-{}^6P_{7/2}$ ($\lambda_1 = 576.5$ nm). The beam from the second laser ionized the atom from the excited state in a two-step process involving two transitions: a resonance transition from the $^6P_{7/2}$ level to the level under study and a transition from this level to the ionization continuum. Since the energy of the laser pulse was insufficient to saturate the transition to the continuum, the quadratic dependence of the ion current on the energy of the laser pulse in the initial region went over to a linear dependence in the saturation region of the resonance transition under study. A sample curve for the ratio of the photoion current to the energy density of the laser pulse is shown in Fig. 3. For the transitions studied we have $\mathscr{E}_{sat} \lesssim 0.2$ mJ/cm² (Table II).

The saturation energies were determined at a laser linewidth $\Delta\nu_L = 0.8$ cm^{-1} which was larger than the absorption linewidth $\Delta\nu_{at} = 0.005$ cm^{-1} in the atomic beam. The emission linewidth of the dye lasers used in the experiment was practically independent of the type of pump laser. Therefore, for a laser-beam diameter $d = 3$ mm and a pulse repetition frequency $f = 10$ kHz, the average saturation power of the second-step transition was

$$P_{sat} = \mathscr{E}_{sat} f \pi d^2/4 \approx 0.1 \text{ W}.$$

An average radiation power of this level is easily realized with dye laseres pumped by a copper-vapor laser.

The lifetime of the first excited state $^6P_{y/2}$ can be estimated using the data of Ref. 30. The resulting value $\tau_1 \approx 1$ μsec is much larger than the duration of the laser pulses. Therefore, the finite lifetime of this state does not affect the excitation kinetics of the atom. The lifetime of the second excited states in europium are not known. We have mea-
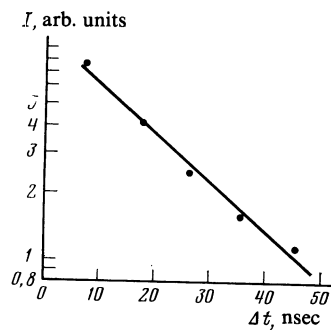
sured the lifetime of several excited states by the following method. Two lasers resonantly excited the state under study. The population of this state varies with time as

$$n_2 = n_{20} \exp(-t/\tau_2). \tag{2}$$

The lifetime of this state was determined by studying how the current of photoions due to the ionization of the excited atoms by the beam of a third laser depends on the optical delay time of the pulse of this laser with respect to the pulse of the second-step laser (Fig. 4). When the delay is longer than the laser pulse ($\tau_L = 7$ ns), a dependence of the type in (2) is found. The results of these measurements are given in Table II. For the method used in these measurements, the uncertainty in the lifetime of the excited state is goverened by the instability of the amplitude of the laser pulses and amounts of ± 2 ns. As can be seen from the data, the condition $\tau_L \lesssim \tau_k$ is not satisifed for all the levels.

On the basis of all the data (the width of the hyperfine structure, the saturation energy of the second transition, the lifetime of the second state, and the relative intensity of the autoionization transitions), we chose the most efficient sequence of atomic transitions in europium for the purpose of measuring the isotope shifts of its radioactive isotopes; this sequence is shown in Fig. 1.

3. MEASUREMENT OF ISOTOPE SHIFTS

The apparatus for measuring the isotope shifts is shown schematically in Fig. 5. Three dye lasers are pumped by two synchronously operating ILGI-101 copper-vapor lasers. The average radiation power of this laser is 5 W in two lines: 510.6 and 578.2 nm. The emission frequency of the first dye laser was tuned over a 0.6 cm^{-1} interval by changing the pressure in the chamber holding the diffraction grating and Fabry-Perot interferometer. The emission linewidth of this laser was $\Delta\nu_L = 0.02$ cm^{-1}. As the frequency of the narrow-band laser was tuned, the europium isotopes were excited sequentially to the $^6P_{7/2}$ state. They were further excited and ionized by two other dye lasers which were tuned to resonance with the chosen transitions. The power of the laser radiation in the first, second, and third excitation steps was 2, 120, and 250 mW, respectively.

The laser beams made a right-angle intersection with two atomic beams produced by two high-temperature ovens[16] located in a single vacuum chamber. Into one oven we placed tantalum foils containing the radioactive isotopes,

TABLE II. Saturation energies $\mathscr{E}_{sat}$ for transitions between excited states and the lifetimes τ for several excited states of Eu I (the initial state was $4f^76s6p\ ^6P_{7/2}$ at 17340.65 cm^{-1}).

| Transition wavelength, nm | Excited state | | | $\mathscr{E}_{sat}$, $\mu J/cm^2$ | τ, ns | $\Delta\tau$, ns |
	configu-ration	term	energy, cm^{-1}			
595.578	—	$3^0_{7/2,\,9/2}$	34126.42	—	53	±3
560.586	$4f^75d^2$	$^8P^0_{5/2}$	35174.20	80	16	±1
557.266	$4f^75d^2$	$^8P^0_{9/2}$	35280.43	140	39	±7
554.254	—	$^8D^0_{7/2}$	35377.94	40	20	±1

and into the other we placed metallic europium. The atomic beam with the stable isotopes ^{151,153}Eu was used as a reference and as an aid for tuning the laser frequencies to the atomic transitions. The diameter of the laser beams was 3 mm and the length of its interaction region with the atomic beam was 8 mm. A portion of the radiation of the narrow-band laser was directed to a confocal interferometer with a free dispersion region of 0.125 cm^{-1}. The selectively produced photoions were extracted by a static electric field ($U \approx 100$ V) in the direction perpendicular to the atomic and laser beams and sent to secondary electron multipliers. The signals from the two secondary electron multipliers and the confocal interferometer were sent to a measurement-computational complex which includes small computers.

Thus as the laser frequency was scanned, three spectra arose: The photoion excitation spectrum of the radioactive isotopes, the photoion excitation spectrum of stable isotopes, and the transmission spectrum of the interferometer. From the two lines of the stable isotopes ^{151,153}Eu we determined the free-dispersion region of the interferometer (from the values of the isotope shifts in Ref. 29), and from the num-

ber of fractional and whole interference fringes we determined the position of the lines belonging to radioactive isotopes relative to the line of the isotope ^{151}Eu. The uncertainty in the measurement of the position of the isotopic lines was 70 MHz and was due to the instability of the lasing linewidth and the nonlinearity of the frequency tuning of the laser.

An electrostatic shield placed above the oven and a coincidence circuit for the laser pulses and photoions decreased the background of nonlaser-produced ions to one pulse per second.

The measurements were made "off-line". The samples were prepared in the following order. Radioactive europium isotopes were obtained by bombarding a 120-g tantalum target with a beam of 1-GeV protons at an intensity of 10^{12} protons/sec on the synchrocyclotron of the Leningrad Institute of Nuclear Physics. The nuclear reaction products were separated from the target at a temperature of 2500°C, ionized on a tungsten surface, and separated on a mass separator with a tantalum target (preliminarily annealed for about 1 h at 2000°C) in the focal plane. A scintillation counter was used to find the areal distribution of the radioactive isotopes driven into the tantalum foil. A Ge (Li) detector was used to measure the quantity of each isotope. After several hours, from 10^{10} to 10^{11} atoms of each isotope had been produced (see Table III).

The part of the foil containing the isotope to be studied was placed in an atomic-source oven. At a temperature of 1300–1500°C practically all the atoms of the isotope had left the foil. In one of the measurement cycles a sample containing $3\cdot10^{10}$ atoms of the isotope ^{145}Eu supported a stable photoionization signal for 12 min, corresponding to a flux of $4\cdot10^7$ atoms/sec. During this time 12 recordings of the spectra were made. A thousand ^{145}Eu photoions were detected in all. On the basis of these data one can estimate the detection efficiency for radioactive Eu atoms in these experiments.

The detection efficiency η is taken to be the ratio of the number of photoions detected to the number of atoms of the investigated isotope originally present in the atomic-beam oven, at a fixed laser frequency tuned to the line center. The value of η was detected from the relation
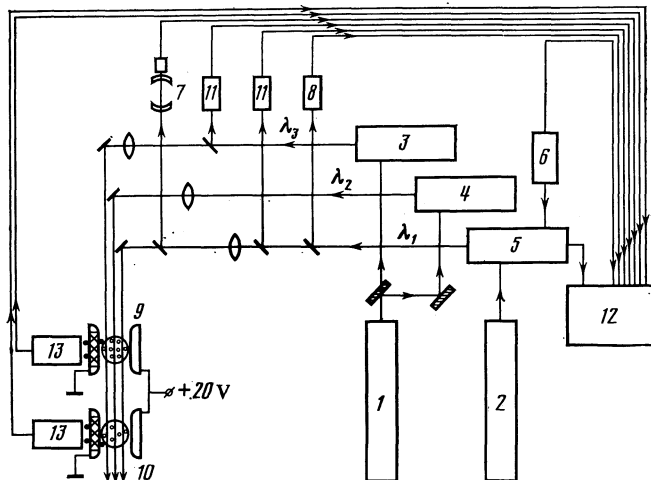

FIG. 5. Schematic of the optical part of the laser apparatus for measuring the isotope shifts and hyperfine structures of radioactive nuclides. 1, 2) copper-vapor lasers, 3, 4) dye lasers, 5) narrow-band dye laser with wavelength tunable by changing the pressure in a chamber containing a diffraction grating and interferometer, 6) control unit for nitrogen pressure in the pressure chamber of the laser, 7) confocal interferometer, 8) monochromator, 9, 10) atomic beams of stable and radioactive isotopes, 11) photodiodes of coincidence circuit, 12) computer-based electronics complex, 13) secondary electron multipliers.

$$\eta = \frac{M}{m}\frac{\tau_0+\tau_1}{\tau_0}\frac{n}{N}, \tag{3}$$

where M is the magnitude of the signal obtained at the maximum of the optical resonance as a result of the evaporation

733   Sov. Phys. JETP 59 (4), April 1984

Zherikhin et al.   733

TABLE III. Relative isotope shifts $\Delta\nu$ in the spectrum of Eu I and the uncertainty $\delta\nu$ in their measurement, the changes in the mean-square charge radius of the nuclei (the measured $\Delta\langle r^2\rangle^{151,A}$ and calculated $\Delta\langle r^2\rangle_0^{151,A}$ values), the deformation parameters $\langle\beta^2\rangle$, the decay half-lives $T_{1/2}$, and the number n of atoms of the isotopes.

A	$\Delta\nu(151-A)$, GHz	$\pm\delta\nu$, GHz	$\Delta\langle r^2\rangle^{151,A}$, fm^2	$\Delta\langle r^2\rangle_0^{151,A}$, fm^2	$\langle\beta^2\rangle^{1/2}$	$T_{1/2}$	$n\cdot 10^{-10}$
154	4.34	0.027	0.744	0.154	0.36	16 yr	—
153	3.619	0.020	0.620	0.103	0.35	—	—
152	3.342	0.024	0.571	0.051	0.35	12.7 yr	—
151	0	0	0	0	0.25	—	—
150	−1.48	0.08	−0,254	−0,051	0,20	12.6 day	—
149	−1.85	0.08	−0,320	−0,102	0,19	93 day	32
148	−2.98	0.08	−0,518	−0,154	0,14	54 day	6
147	−3.39	0.08	−0,586	−0,205	0,14	22 day	10
146	−4,19	0,10	−0,725	−0,256	0,09	4.6 day	1.7
145	−4,90	0.10	−0,820	−0,307	0.0	5.9 day	3

of all the atoms of the isotope from the sample, m is the magnitude of the signal from a single ion, τ_0 is the time over which the spectrum is obtained, τ_1 is the return time, n is the number of channels used in recording the spectrum, and N is the number of atoms of the isotope in the foil. An averaging of the data for eight series of measurements (one series for each foil) yielded the following estimate for the detection efficiency of an isotope: $\eta = 6\cdot10^{-6}$.

The comparatively low value of the detection efficiency obtained here can be attributed to the following effects. The collimation of the atomic beam was such that around 1% of the atoms leaving the source entered the ionization region. In addition, losses arise because some of the atoms intersect the ionization region during the gap between laser pulses. The interception coefficient K is

$$K = df/v \approx 0.06, \tag{4}$$

where v is the average thermal speed of the atoms. We must also take into account the losses due to the incomplete evaporation of the atoms from the foil, the incomplete extraction of the photoions from the photoionization region, and the less-than-100% efficiency of the secondary electron multipliers. The efficiency of the photoionization of isotopes by the laser radiation amounted to 1% and was governed mainly by the degree of saturation of the autoionization transition.

Even at the low detection efficiency achieved we were able to measure the hyperfine structure and isotope shift with rather small fluxes of radioactive atoms. In fact, the center of the optical line is determined to an accuracy of 80 MHz with only 10 atoms detected at the maximum. This means that when working with a continuous flux of isotopes one needs just 10^7 ions/sec to obtain the spectum during the scanning time of the laser frequency, i.e., in 20 sec.

Table III gives the measured isotope shifts (relative to ^{151}Eu) for isotopes with mass numbers from $A = 145$ to $A = 154$.

4. DISCUSSION OF RESULTS

The isotope shift $\Delta\nu^{AA'}$ in the spectra of heavy atoms is well described by the familiar formula

$$\Delta\nu^{AA'} = b\lambda^{AA'} + \Delta\nu_M, \tag{5}$$

where b is a coefficient reflecting the change in the wave function of the atom, $\lambda^{AA'}$ is a factor determined by the charge distribution in the nucleus, and $\Delta\nu_M$ is the specific mass shift.

The transitions between configurations $6s^2$ and $6s6p$ in Eu I can be regarded as transitions between pure configurations.[32] For such transitions $\Delta\nu_M$ can be estimated in the standard way[33]:

$$\Delta\nu_M = \frac{\nu_0}{1836}(1\pm0.5)\frac{A-A'}{AA'}, \tag{6}$$

where ν_0 is the transition frequency, and A and A' are the atomic numbers of the isotopes in question. This estimate is in good agreement with theoretical calculations of the mass shift and with a calibration of the optical shifts using the x-ray and muon-atom shifts for the neighboring element.[34]

To evaluate the change in the electron density at the nucleus, $|\psi(0)|^2$, and to find the coefficient b, one uses the Goudsmit-Fermi-Segrè formula relating $|\psi(0)|^2$ to the energy of the level of the $nS_{1/2}$ series in the atom under study or in an ion given atom and the formula relating $|\psi(0)|^2$ to the magnetic hyperfine-splitting constant A_{ns} for the ns electron. We used published data on a_{ns} for the configuration $4f^76s6p$ (Ref. 35) and $4f^75d\,6s$ in Eu I and $4f^76s$ in Eu II (Ref. 37), and also the data of Ref. 38 for the series $4f^7$ in Eu II and $4f^75dns$ in Eu I. Averaging all the values obtained for b, we have $\bar{b} = 6.12(30)$ GHz/fm^2, where the error indicated is the mean-square deviation.

The factor $\lambda^{AA'}$ is expressed in the form of a series:

$$\lambda^{AA'} = \Delta\langle r^2\rangle\left(1 + C_1\frac{\Delta\langle r^4\rangle}{\Delta\langle r^2\rangle} + C_2\frac{\Delta\langle r^6\rangle}{\Delta\langle r^2\rangle} + \ldots\right). \tag{7}$$

The coefficients C_1 and C_2 are small and have been tabulated in Ref. 39. In the simplest liquid-drop model with a uniform charge distribution and an abrupt edge we have the relation

$$\Delta\langle r^2\rangle^{AA'} = \lambda^{AA'}/0.958. \tag{8}$$

The droplet model of Myers and Swiatecki[40] gives a quantitative description of the nuclear masses and dimensions over the entire periodic table. Although the droplet model has recently come under serious criticism,[41] it turns out that it gives only uneventful discrepancies with the results of Hartree-Fock calculations for the nuclear properties which depend on the change of the basic model parameters ε
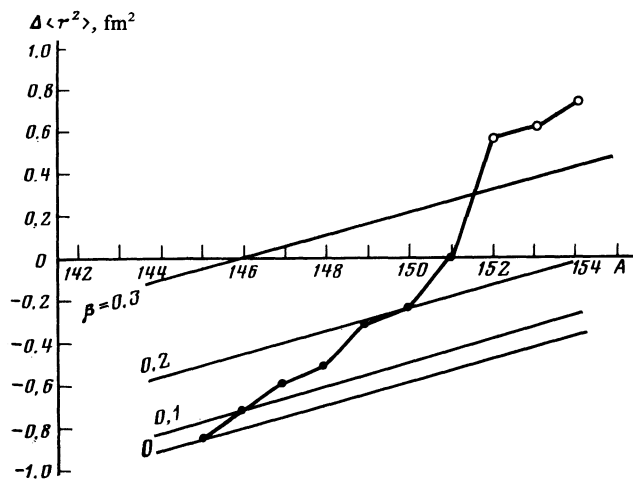
FIG. 6. Mass-number dependence of the change, relative to ^{151}Eu, in the mean-square radius of the nuclear charge distribution for europium isotopes (β is the deformation parameter calculated in the droplet model of the nucleus); the open circles are the data of Ref. 33.

and δ with the atomic number A. Therefore, for treating the isotope shifts the droplet model is entirely suitable.

Table III gives the calculated results $\Delta \langle r^2 \rangle_0^{151,A}$ for the isotopic changes of the mean-square charge radius in the droplet model. The uncertainty in the calculation of $\Delta \langle r^2 \rangle$ is 5%. The calculated and experimental data can be used to determine the mean-square deformation of the nuclei by introducing the deformation parameter β into the droplet model. The results of a calculation under the assumption $\langle \beta^2 \rangle = 0$ for ^{145}Eu are also given in Table III.

The results are also presented in Fig. 6. The smooth growth of $\langle \beta^2 \rangle$ for the nuclei $^{145-151}$Eu is evidence of a gradual growth in the deformation on approaching the nucleus ^{151}Eu, with neutron number $N = 88$, in confirmation of the conclusions of Ref. 22. An even-odd effect, leading to a relative decrease of $\langle \beta^2 \rangle$ for odd-neutron nuclei, is clearly seen. A knee, corresponding to a sharp growth in the deformation of the nucleus, appears on the curve of the mean-square charge radius at ^{152}Eu. On the whole, the change in the mean-square charge radius with increasing N for Eu isotopes corresponds to the change in the mean-square charge radius for neighboring elements Gd and Sm and differs markedly from the behavior of the mean-square charge radius in the $N = 90$ region for Ba and Yb, for which the curves do not exhibit the characteristic knee.[10] This can be regarded as confirmation of the hypothesis that the proton shell $Z = 64$ has a stabilizing influence which leads to the abrupt growth of the deformation for nuclei with nearby values of Z ($Z = 63$ for Eu; $Z = 62$ for Sm), in contrast with the smooth dependence of β on N for nuclei far from this shell ($Z = 70$ for Yb; $Z = 56$ for Ba).[7] Of particular interest is the fact that our results were obtained for odd-proton nuclei, while all the previously available data pertained only to even-proton nuclei of the transition region.

A deeper understanding of the data can be attained by invoking models which describe the entire body of experimental data, not only for the dimensions of the nuclei but also their spectra, transition probabilities and electromag-

netic moments. One such model is the dynamic collective model.[42] This model has been used successfully to describe the change in the mean-square charge radius iostopes of Cs and Hg. Another attractive feature is that the mean-square charge radius can be calculated in this model without introducing new parameters, unlike the case for most models of this sort. Computer calculations have yielded a relatively good description of the energy spectra of the nuclei $^{145-151}$Eu. Sataisfactory agreement with experiment is also obtained for the lifetime of certain levels. However, despite the satisfactory description of the spectroscopic characteristics of the isotopes of Eu, the change in the mean-square charge radius has not yet been described satisfactorily with the same parameters.

5. CONCLUSIONS AND OUTLOOK

Our results point up the particular importance of data on the mean-square radius for refining the existing nuclear models, since they demonstrated the sensitivity of the mean-square charge radius to details of the nuclear structure. In this case we have apparently discovered a new mechanism, not incorporated in the model, which leads to suppression of the effective forces for the nuclei under study. Allowance for the high multipolarity of the zero-point vibrations and considerations of the influence of the zero-point vibrations on superfluidity in the framework of this model can improve the agreement between the theoretical and experimental values, as is evidenced by the results of Ref. 43.

Let us also discuss the possibility of improving the sensitivity and accuracy of the measurements of the isotope shifts. The average radiation power of the dye laser in the photoionization step can be increased to 1 W using a dye amplifier.[25] This gives a four-fold increase in the yield. Because of the insignificant density of atoms in the beam, the laser radiation is not absorbed and can therefore be used many times with the aid of a multipass system consisting of mirrors, for example. It is entirely possible to pass the laser beam through the atomic beam 25–30 times. The ionization efficiency can thus be increased by two orders of magnitude to 10^{-4}, making it possible to study isotope fluxes of 10^5 atoms/sec. The use of a dye laser with a lasing linewidth $\Delta v_L = 0.005$ cm^{-1} and a smooth, well-reproducible line shape will permit a four-fold increase in the resolution and an improvement in the accuracy of measurement of the isotope shifts to 20 MHz.

A noticeable gain in the sensitivity of the apparatus for studying short-lived isotopes can be realized in "on-line" operation, when, for example, the atomic-beam oven is mounted in line with the ion beam split off by the mass separator. This eliminates the stage of working with the isotopes in air. Preliminary experiments showed that in this case the background of stable isotopes from the foil material and the oven structures can be practically eliminated.

A substantial increase in the efficiency of the whole laser-nuclear complex can be obtained by arranging the photoionization of the isotopes directly at the exit from the target. In this case the laser photoionization serves as the ion source in place of a conventional source using surface-ioni-

zation or gas discharge, etc. The efficiency of the mass separator with such a source increase by 10–100 times, depending on the element.

In such a version the laser-nuclear complex can be used to obtain beams of single isomeric nuclei and single isotopes, without isobaric impurities. Such beams are necessary in a number of nuclear experiments involving isomers and can also be used in other experiments, for example, in precise measurements of the isotope masses.

We wish to thank V. E. Mitroshin and G. B. Krygin for providing a computer program for the dynamic collective model and for helpful discussions.

[1]The preliminary results of this study were published in Ref. 1.

[1]G. D. Alkhazov, A. E. Barzakh, É. E. Berlovich et al., Pis'ma Zh. Eksp. Teor. Fiz. 37, 231 (1983) [JETP Lett. 37, 274 (1983)].
[2]H. J. Kluge, R. Neugart, and E.-W. Otten, in: Laser Spectroscopy IV (H. Walter and K. W. Rothe, eds.), Proc. Intern. Conf., Rottach-Egern, FRG, June 11–15, 1979, Springer-Verlag, Berlin (1979), p. 517.
[3]G. Huber, C. Thibault, R. Klapisch et al., Phys. Rev. Lett. 34, 1209 (1975).
[4]C. Thibault, F. Touchard, S. Büttgenbach et al., Phys. Rev. C 23, 2720 (1981).
[5]T. Kuhe, P. Dabkiewicz, C. Duke et al., Phys. Rev. Lett. 39, 180 (1977).
[6]F. Buchinger, P. Dabkiewicz, H. J. Kulge et al., Hyperfine Interactions 9, 165 (1981).
[7]H. J. Kluge, H. Kremmling, H. A. Schissler et al., Z. Phys. A 309, 187 (1983).
[8]J. Nowicki, K. Bekk, S. Göring et al., Phys. Rev. C 18, 2369 (1978).
[9]R. C. Thompson, A. Hauser, K. Bekk et al., Z. Phys. A 305, 89 (1982).
[10]R. Neugart, Proc. Conf. on Lasers in Nuclear Physics (C. E. Bemis and H. C. Carter, eds.), Harwood Academic Publ., Chur, London, New York (1982).
[11]E.-W. Otten, Nucl. Phys. A 354, 471 (1981).
[12]Proc. Conf. on Lasers in Nuclear Physics (C. E. Bemis and H. C. Carter, eds.), Harwood Academic Publ., Chur, London, New York (1982).
[13]V. S. Letokhov, V. I. Mishin, and A. A. Puretskiĭ, in: Khimiya Plazmy [Plasma Chemistry], No. 4, Atomizdat, Moscow (1977).
[14]N. V. Karlov, B. B. Krynetskiĭ, V. A. Mishin, and A. M. Prokhorov, Usp. Fiz. Nauk 127, 593 (1979) [Sov. Phys. Usp. 22, 220 (1979)].
[15]G. S. Hurst, M. G. Payne, S. D. Kramer, and T. P. Young, Rev. Mod. Phys. 51, 767 (1979).
[16]V. I. Balykin, G. I. Bekov, V. S. Letokhov, and V. I. Mishin, Usp. Fiz. Nauk 132, 293 (1980) [Sov. Phys. Usp. 23, 651 (1980)].
[17]G. I. Bekov, V. S. Letokhov, O. I. Matveev, and V. I. Mishin, Pis'ma Zh. Eksp. Teor. Fiz. 28, 308 (1978) [JETP Lett. 28, 283 (1978)].
[18]G. I. Bekov, V. S. Letokhov, and V. I. Mishin, Zh. Eksp. Teor. Fiz. 73, 157 (1977) [Sov. Phys. JETP 46, 81 (1977)].
[19]E. Ye. Berlovich, E. I. Ignatenko, and Yu. N. Novicov, Proc. Eighth Intern. EMIS Conf., Skövele, Sweden (1973), p. 349.
[20]É. E. Berlovich, L. Kh. Batist, Yu. S. Blinnikov et al., Izv. Akad Nauk SSSR Ser. Fiz. 40, 2036 (1976).
[21]É. E. Berlovich, Izv. Akad Nauk SSSR Ser. Fiz. 43, 2046 (1979).
[22]É. E. Berlovich, Izv. Akad Nauk SSSR Ser. Fiz. 29, 2177 (1965).
[23]G. A. Linder and P. Möler, Phys. Lett. B. 110, 17 (1982).
[24]V. S. Letokhov, Nelineĭnye Selektivnye Fotoprotsessy v Atomakh i Molekulakh [Nonlinear Selective Photoprocesses in Atoms and Molecules], Ch. 3 and 7, Nauka, Moscow (1983).
[25]A. N. Zherikhin, V. S. Letokhov, V. I. Mishin et al., Kvantovaya Elektron. (Moscow) 8, 1340 (1981) [Sov. J. Quantum Electron. 11, 806 (1981)].
[26]V. I. Mishin, V. E. Mnuskin, V. G. Nikiforov et al., Prib. Tekh. Eksper., No. 2, 246 (1983).
[27]W. L. Martin, R. Zalubas, and L. Hagan, Atomic Energy Levels. The Rare-Earth Elements, NSRDS-NBS 60, Washington, D. C. (1978).
[28]G. I. Bekov, V. S. Letokhov, and V. I. Mishin, Zh. Eksp. Teor. Fiz. 73, 157 (1977) [Sov. Phys. JETP 46, 81 (1977)].
[29]G. J. Zaal, W. Hagervarst, E. R. Eliel et al., Z. Phys. A 290, 339 (1979).
[30]C. H. Corliss and W. R. Bozeman, Experimental Transition Probabilities for Spectral Lines of Seventy Elements . . . , U. S. Government Printing Office, Washington, D. C. (1962).
[31]R. V. Ambartsumyan, A. M. Apatin, V. S. Letokhov et al., Zh. Eksp. Teor. Fiz. 70, 1660 (1976) [Sov. Phys. JETP 43, 866 (1976)].
[32]F. Smith and B. J. Wybourne, J. Opt. Soc. Am. 55, 121 (1965).
[33]K. Heilig and A. Steudel, At. Data Nucl. Data Tables 14, 613 (1974).
[34]H.-W. Brandt, E. Meissner, and A. Steudel, Z. Phys. A 291, 97 (1979).
[35]E. R. Ehell, K. A. H. Van Zeenwen, and W. Hagervarst, Phys. Rev. A 22, 1491 (1980).
[36]H.-W. Brandt et al., Z. Phys. A 302, 291 (1981).
[37]G. Guthörlein, Z. Phys. 214, 332 (1968).
[38]J. Sugar and J. Reader, J. Opt. Soc. Am. 55, 1286 (1965).
[39]E. C. Selzer, Phys. Rev. 188, 1916 (1969).
[40]W. D. Myers and W. J. Swiatecki, Ann. Phys. (N. Y.) 55, 395 (1969).
[41]F. Tondeur, J. M. Pearson, and M. Farine, Nucl. Phys. A 394, 462 (1983).
[42]V. E. Mitroshin, Preprint LIYaF-441, Leningrad Institute of Nuclear Physics (1978).
[43]V. E. Mitroshin, Preprint LIYaF-214, Leningrad Institute of Nuclear Physics (1976).

Translated by Steve Torstveit